Solution Structure of Human Brg1 Bromodomain and Its Specific Binding to Acetylated Histone Tails[†,‡]

Weiqun Shen, Chao Xu, Wei Huang, Jiahai Zhang, Justin E. Carlson,[§] Xiaoming Tu, Jihui Wu,* and Yunyu Shi*

School of Life Sciences, and Hefei National Laboratory for Physical Sciences at Microscale, University of Science and Technology of China, Hefei, Anhui, 230026, People's Republic of China

Received June 6, 2006; Revised Manuscript Received November 30, 2006

ABSTRACT: Human brahma-related gene 1 (Brg1) is a core protein in human SWI/SNF chromatin-remodeling complex which regulates gene expression. Brg1 contains a bromodomain that has been shown to anchor the entire complex to promoter nucleosomes by interacting with histones that are acetylated at specific lysine residues. The Brg1 bromodomain belongs to an important subclass of the bromodomain family for which no structural information is known. Here we report the solution structure of the Brg1 bromodomain determined by NMR. The Brg1 bromodomain conserves the left-handed, four-helix bundle topology found in other bromodomain structures. However, the αZ helix of Brg1 bromodomain is about 4 residues shorter relative to previously published bromodomain structures. Using NMR perturbation studies, we demonstrate the Brg1 bromodomain binds acetyllysine in the context of histone tails, with no comparable affinity for unacetylated peptides. The estimated dissociation constants (K_D) for acetylated histone peptides H4−AcK8 and H4−AcK12 are 4.0 and 3.6 mM, respectively. In this study the dominant substrate was H3−AcK14 ($K_D \approx 1.2$ mM). Mutagenesis analysis reveals several residues important for the binding specificity. Using molecular dynamics simulations, we present a model of the Brg1 bromodomain in complex with H3−AcK14 and discuss the potential interactions which provide the selectivity of the Brg1 bromodomain for histone H3−AcK14.

Chromatin remodeling plays an important role in the activation and regulation of eucaryotic gene expression. There are two main groups of ATP-dependent chromatin-remodeling complexes, the SWI2/SNF2 group and the imitation SWI (ISWI) group (*1*). The SWI2/SNF2 group includes yeast SWI/SNF (ySWI/SNF), yeast RSC, the *Drosophila* Brahma complex, and the human Brahma (hBRM) and Human brahma-related gene 1 (Brg1) complexes (*2*). This group of complexes was first discovered in yeast by genetic screening for altered expression of the two genes SWI and SNF (*3*−*5*). Subsequently, SWI/SNF homologues were found in *Drosophila* and human (*6*, *7*). SWI2/SNF2 complexes help activate gene transcription by disrupting nucleosome structure at promoters and facilitating the binding of transcription factors to their cognate sites (*8*). Brg1 or hBRM is the core catalytic subunit of human SWI/SNF complex, and Brg1 alone can substitute for the core complex, albeit with less efficiency (*1*). Brg1 shares 73% sequence identity with hBRM. Their functions are redundant to a certain level, but they play different roles in cellular proliferation and differentiation (*9*). Both proteins contain an evolutionarily conserved ATPase domain, which is the catalytic module, and a conserved bromodomain, which is responsible for anchoring the protein or the complex to acetylated promoter nucleosomes (*10*). Their bromodomains differ by only one amino acid. The sequence identity of bromodomains within the SWI2/SNF2 subfamily is above 27% and no structures of these bromodomains from the SWI2/SNF2 subfamily have been reported.

Recent studies have shown that Brg1 regulates the expression of a variety of genes either as the core member of SWI/SNF complex or by associating with other proteins. The genes Brg1 affects are involved in multiple cellular processes including cell proliferation, cell differentiation, and tumor suppression (*11*−*13*). Reintroduction of Brg1 into a breast tumor cell line carrying a defined mutation in the Brg1 gene induces growth arrest by down regulation of certain E2F target genes such as cyclin E, cyclin A, and CDC2 (*14*, *15*). More dramatically, reintroduction of Brg1 up-regulates CDK inhibitors p21 and p15 (*13*). Accumulating molecular genetic evidence suggests that ATP-dependent chromatin remodeling by the SWI/SNF complex plays a crucial role in human tumorigenesis. The gene encoding Brg1 was found to be mutated in human tumor cell lines from various tissues including prostate, lung and breast (*16*, *17*). Murphy et al. demonstrated that Brg1 represses transcription of the oncogene c-FOS in an E2F-independent manner (*18*), and recent

[†] This work was supported by the Chinese National Fundamental Research Project (Grant G1999075605, 2002CB713806, 2006CB806500), the Chinese National Natural Science Foundation (Grants 30270293 and 30121001), the Key Project of the National High Technology Research and Development Program of China (Grant 2002BA711A13), and the Pilot Project of the Knowledge Innovation Program of the Chinese Academy of Science (Grant KSCX1-SW-17).

[‡] The atomic coordinates have been deposited in the RCSB Protein Data Bank with accession code 2H60.

* To whom correspondence should be addressed. Tel: +86-551-3607464. Fax: +86-551-3601443. E-mail: yyshi@ustc.edu.cn (Y.S.), wujihui@ustc.edu.cn (J.W.).

[§] Present address: The Scripps Research Institute, The Laboratory of Prof. Ian A. Wilson, D. Phil., Department of Molecular Biology, 10550 North Torrey Pines Rd., BCC206, La Jolla, CA 92037.

10.1021/bi0611208 CCC: $37.00
Published on Web 02/03/2007

work from Strobeck et al. suggested that Brg1 regulates CD44 expression, which encodes a transmembrane glycoprotein relevant to tumor growth and metastasis (*19*). Brg1 is also important for T-cell development as T cell-specific Brg1-deficient mice show profound thymic abnormalities, CD4 derepression at the double negative (DN; $CD4^-CD8^-$) stage, and a developmental block at the DN to double positive (DP; $CD4^+CD8^+$) transition (*20*). Despite Brg1's involvement in so many biological processes, the molecular determinants of the critical interactions which recruit the Brg1 complex to specific promoters remain unknown.

Brg1, like other coactivator proteins such as CBP and P/CAF, contains a C-terminal bromodomain. The Brg1 bromodomain is implicated in linking Brg1 protein complexes to chromatin (*21*). During apoptosis, cathepsin G cleaves Brg1 and separates its bromodomain from its helicase activity (*22*). These studies imply the importance of the Brg1 bromodomain to Brg1 function. Bromodomains were originally discovered, and classified as a three helix motif, in the Brahma, the *Drosophila* homologue of Brg1 (*23*). Subsequent analysis verified a fourth, more variable Z helix to the amino terminus of helix A and described a curious link between bromodomains and coactivator proteins (*24*). Structure function studies of the P/CAF bromodomain verified the 4-helical bundle with an unusual left-handed topology and an even more striking acetyllysine binding function (*25*). Extensive studies have come to show bromodomains specifically interact with acetylated lysines (*23*). According to Jeanmougin et al., bromodomains are classified into 7 groups (*24*). The Brg1 bromodomain represents group I bromodomains which are associated with ATPase associate chromatin-remodeling activity.

Together with other modifications, such as methylation, phosphorylation, sumolyzation, and ubiquitination, histone acetylation forms the histone code, a complex modification language that is fundamental to the regulation of chromatin structure and function (*26*, *27*). Multiple histone acetylation sites set the stage for temporal and spatial recruitment of chromatin-remolding complexes and transcription factors. Bromodomains from different proteins recognize different sets of histone code. Specific recognition of acetylated histones by bromodomains implicates their roles in epigenetic memory (*28*). Theodora et al. reported that acetylation of histone H4 K8 mediates recruitment of the SWI/SNF complex during IFN-β gene activation (*29*). It is not clear if the same histone acetylation code is utilized in other Brg1-dependent gene activations.

Here we report the solution structure of Brg1 bromodomain, as determined by NMR experiments, and its specific binding to acetylated histone H4 and H3 tails. Using molecular dynamics simulations, we demonstrate potential interactions in a modeled Brg1 bromodomain H3−AcK14 complex. Combining the model with experimental data, we discuss the molecular interaction which could provide the Brg1 bromodomain selectivity for histone H3−AcK14 over other acetylated substrates.

MATERIALS AND METHODS

Expression, Purification, and Isotope Labeling of Brg1 Bromodomain. The DNA fragment encoding amino acid residues 1452−1570 of human Brg1 was amplified by polymerase chain reaction from human brain cDNA library (Clontech) using specific primers (5′-CATATGTCCCCTAACCCAC-3′ and 5′-CTCGAGACTGTCATCCTCCT-3′). This amplified DNA fragment was cloned into the plasmid pET22b (+) (Novagen), using restriction enzymes *Nde* I and *Xho* I. Sequencing verified the construct to be identical to 1452−1570 of human Brg1 (gene bank code U29175). After induction of and harvesting of *E. coli* BL21 (DE3) (Stratagene) transformed with the expression vector, 35 mg of Brg1 bromodomain per liter was obtained. Uniformly ^{15}N- and ^{13}C-labeled recombinant proteins were produced by growing BL21 (DE3) bacteria in SV40 medium using ^{15}-NH_4Cl (0.5 g/L) and glucose-$^{13}C_6$ (2.5 g/L) as stable isotope sources. Recombinant bromodomain fragment was purified by Hi-trap chelating column (Pharmacia) chromatography and size-exclusion chromatography on Superdex 16/60 column (Pharmacia). The purified recombinant protein construct contains amino acid residues 1452−1570 from Brg1, an amino terminal methionine and a carboxyl terminal histidine tag (-LEHHHHHH) which is encoded by the pET22b (+) expression vector. The purity of the bromodomain was confirmed by SDS-PAGE, and the concentration was estimated with BCA reagent (Pierce).

Peptide Synthesis and Purification. The peptides of acetylated histone tails H4−AcK8 (residues 1−12 of histone H4, SGRGKGG-AcK-GLGK), H4−AcK12 (residues 7−17 of histone H4, GKGLG-AcK-GGAKR), H4−AcK16 (residues 13−20 of histone H4, GGA-AcK−RHRK), H2B-AcK5 (residues 1−12 of histone H2B, SDPA-AcK-SAPAPKK), H3−AcK14 (residues 9−18 of histone H3, KSTGG-AcK-APRK), H3−R17/A (Arg 17 to Ala mutation of H3−AcK14, KSTGG-AcK-APAK), and the unacetylated histone H4 peptide (residues 1−12 of histone H4, SGRGKGGKGLGK) were chemically synthesized using a standard Fmoc (*N*-9-fluorenyl methoxycarbonyl) method at Shanghai Sangon Biological Engineering & Technology and Service Co. Ltd. AcK is lysine acetylated at the ϵ-NH_2. The synthetic peptides were purified by reverse-phase high-pressure liquid chromatography (C18 column), eluted with a linear gradient, 15−30%, of acetonitrile. The final product was lyophilized and verified by matrix-assisted laser desorption ionization time-of-flight (MALDI-TOF) mass spectrometry.

NMR Experiments. NMR samples of 1−1.5 mM Brg1 bromodomain were buffered in 25 mM sodium phosphate (pH 6.4), 100 mM NaCl, 1 mM EDTA, and 5 mM DTT in 90% H_2O, 10% D_2O in 500 μL. We acquired NMR spectra at 293 K, using a Bruker DMX600 spectrometer with self-shielded *z*-axis gradients. To obtain backbone and side chain resonance assignments, the following spectra were recorded: 2D $^1H-^{15}N$ HSQC, 3D triple-resonance spectra HNCO, HN(CA)CO, CBCA(CO)NH, CBCANH, C(CO)NH-TOCSY, H(CCO)NH-TOCSY, ^{15}N-TOCSY, HCCH-TOCSY, HCCH-COSY, HBHA(CBCACO)NH. 3D ^{15}N-separated and ^{13}C-separated NOESY were acquired with mixing time of 100 and 130 ms, respectively. To identify the slowly exchanging amides, a ^{15}N-labeled sample was lyophilized and dissolved in 99.96% D_2O, followed immediately by HSQC experiments to record the disappearance of NH signals at 293 K. NMR data processing was carried out by NMRPipe software and NMRDraw software, and the data were analyzed using Sparky 3.

Experimental Restraints and NMR Structure Calculation. NMR distance restraints were determined from 3D ^{15}N-edited NOESY and 3D ^{13}C-edited NOESY spectra. NOE restraints were grouped into distance ranges according to their relative intensity: strong (1.8−3.0 and 1.8−3.5 Å), medium (1.8−4.0 and 1.8−4.5 Å), weak (1.8−5.0 Å), and very weak (1.8−5.5 and 1.8−6.0 Å). Considering that the spin diffusion effect could be serious for aliphatic and aromatic protons, a more conservative distance estimation was used for the 3D ^{13}C-separated NOESY. Therefore, most medium-range and long-range NOEs from this spectra were put into the weak or very weak groups whereas most intra-residue NOEs were discarded. The 1.8 Å lower limits were imposed implicitly by the van der Waals repulsion force. For methyl protons, nonstereospecifically assigned methylene protons and aromatic ring protons, r^{-6} summation averages were used.

The TALOS (torsion angle likelihood obtained from shift and sequence similarity) (*30*) was calculated for five types of nuclei: ^{13}Cα, ^{13}Cβ, ^{13}CO, ^{1}Hα, and ^{15}N. Only TALOS "good" predictions, with 9 or 10 matches in agreement, were used and converted into restraints on φ and ψ angles. Hydrogen bond restraints were obtained by identifying the slow-exchange amide protons after 12 h incubation following solvent exchange. For each hydrogen bond, two distance restraints were used: 2.4 Å for H^N-O and 3.3 Å for N−O. Structures were calculated using the program CNS v1.1, employing a simulated annealing protocol for torsion angle dynamics (*31*). The calculated structures were analyzed by the programs PROCHECK (*32*) and MOLMOL (*33*).

NMR Titration. NMR titrations of the Brg1 bromodomain with peptide ligands were performed on 450 μL of 300 μM ^{15}N-labeled protein. Peptide ligand stock solutions of 60 mM in identical buffer were titrated stepwise to a 20:1 peptide to Brg1 bromodomain ratio with a sample dilution of less than 10%. At each titration point, a ^{1}H, ^{15}N-HSQC spectra was acquired at 293 K, using a Brucker DMX600 spectrometer with self-shielded *z*-axis gradients. Combined chemical shift perturbation was calculated using the following equation:

$$\Delta\delta_{ppm} = \sqrt{(\Delta\delta_{HN})^2 + (\Delta\delta_N\alpha_N)^2} \quad (1)$$

where $\Delta\delta_{HN}$ and $\Delta\delta_N$ are the chemical shift variations in the proton and nitrogen dimensions, respectively. α_N, a scaling factor of 0.17, was used to normalize the ^{1}H and ^{15}N chemical shifts (*34*).

Measurement of Equilibrium Dissociation Constants. Dissociation constants, for the interaction of Brg1 bromodomain with different peptide ligands, were obtained by monitoring the chemical shift changes of Brg1 bromodomain from the apo to peptide-bound form during titration with peptide stock. When the exchange rate is greater than the chemical shift difference between the free and bound states, the observed chemical shift at each titration point, δ_{av}, is a weighted average between the chemical shifts of the free and bound states (*35*−*37*) obtained by

$$\delta_{av} = \frac{[P_B]}{[P_T]}\delta_B + \left(1 - \frac{[P_B]}{[P_T]}\right)\delta_F \quad (2)$$

where δ_F is the chemical shift of the protein domain in the absence of a ligand, δ_B is the chemical shift of the protein domain bound to a ligand, $[P_B]$ is the concentration of Brg1 bromodomain bound to a ligand, and $[P_T]$ is the total concentration of Brg1 bromodomain. The mole fraction of the ligand was calculated at each titration point and the titration curve was fitted to calculate the dissociation constant using eq 2 and 3. In eq 3, K_D is the dissociation constant, and $[S_T]$ is the total ligand concentration at each titration point.

$$[P_B] = \frac{1}{2}\{(K_D + [S_T] + [P_T]) - [(K_D + [S_T] + [P_T])^2 - 4[S_T][P_T]]^{1/2}\} \quad (3)$$

Molecular Modeling of Brg1 Bromodomain in Complex with H3−AcK14. To model the Brg1 bromodomain in complex with H3−AcK14, we aligned the Brg1 bromodomain to the *sc*GCN5 bromodomain in complex with acetylated histone H4−AcK16 (PDB ID 1E6I) using CE (*38*) algorithm followed by molecular replacement. We then modeled the H3−AcK14 as H4−AcK16. Side chain positions for H3−AcK14 was determined by searching the backbone-dependent rotamer library (*39*). This composite model of a Brg1 bromodomain H3−AcK14 peptide complex was optimized by molecular dynamics (MD) simulations using the GROMOS96 package (*40*). The GROMOS96 force field combined with an implicit generalized-Born/solvent accessible surface area (GBSA) solvent model was used to perform the simulations. The complex was optimized by 1000 steps of steepest-descent energy minimization. Then during a 300 ps MD simulation at 300 K, all backbone heavy atoms were restrained to their respective starting positions by a harmonic potential restraint force constant of 5.0×10^3 kJ/(mol·nm^2). Another 500 ps MD simulation was performed on the heavy atoms of Brg1 bromodomain residues found outside of the H3−AcK14 binding site, including residues 1482−1490, 1495−1502, 1535−1542, and 1544−1548. The entire Brg1-bromodomain H3−AcK14 complex was optimized by 500 ps MD simulation without any subsequent restraining. Finally, the resulting configuration was minimized through stepwise simulated annealing where during a 400 ps simulation, the temperature of the system was gradually reduced from 300 to 100 K.

Preparation and Characterization of Brg1 Bromodomain Mutants. Mutations were generated by conventional PCR method using Brg1 bromodomain-containing pET22b (+) plasmid as template. For the Val 1484 to Ala (V1484/A) Mutation the following primers were used: 5′-GTCAGCTCAGCGAGGCCTTCATCCAGCTGCCCTC-3′ and 5′-GAGGGCAGCTGGATGAAGGCCTCGCTGAGCTGAC-3′. For the Phe 1539 to Ala (F1539/A) Mutation the following primers were used: 5′-AGAACGCACAGACCGCCAACCTGGAGGGCTCCCT-3′ and 5′-GGGAGCCCTCCAGGTTGGCGGTCTGTGCGTTCTG-3′. For the Asn 1540 to Ala (N1540/A) Mutation the following primers were used: 5′-GAACGCACAGACCTTCGCCCTGGAGGGCTCCCTG-3′ and 5′-CAGGGAGCCCTCCAGGGCGAAGGTCTGTGCGTTC-3′. Mutations were verified by sequencing. BL21 (DE3) cells were transformed with mutagenized Brg1 bromodomain expression plasmids and uniformly ^{15}N-labled mutant proteins were produced as described in previous section. The integrity of Brg1 bromodomain mutants were assessed by their ^{15}N-HSQC spectra. The amide ^{1}H/^{15}N

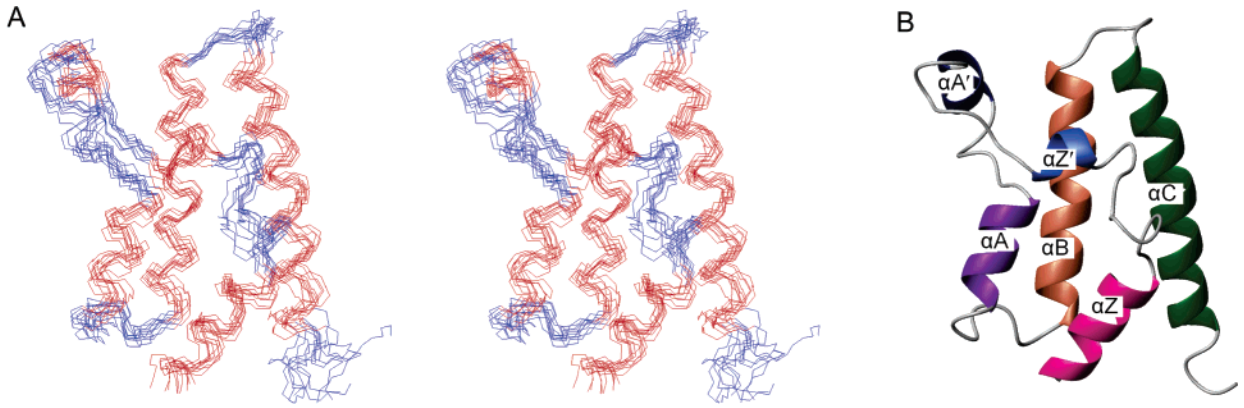

FIGURE 1: NMR structure of Brg1 bromodomain. (A) Stereoview of the Cα trace of 10 superimposed NMR derived structures of the Brg1 bromodomain including residues 1461 to 1570. The disordered amino terminal (1452−1560) and the histidine tag were omitted for clarity. Helices are red and loop regions are blue. (B) Ribbon representation of the average, energy-minimized structure. Secondary structure elements in residues 1461−1471, 1507−1515, 1522−1539, and 1545−1565 correspond to the αZ, αA, αB, and αC helices, respectively. In the ZA loop, short helical elements in residues 1483−1486 and 1495−1500 correspond to αZ′ and αA′ respectively. This figure was produced with MOLMOL (*33*).

resonance line width of each Brg1 bromodomain mutant V1484/A, F1539/A and N1540/A was comparable to that of wild type, indicating the structural stability of each mutant (Shen personal communication).

RESULTS

NMR Structure Determination of Brg1 Bromodomain. A low-resolution structure of Brg1 bromodomain, including residues 1452−1570 was determined by multidimentional heteronuclear NMR spectroscopy. A total of 1355 experimentally derived distance and dihedral angle restraints were utilized in structure calculation (Supporting Information, SI-1). A total of 100 conformers were calculated, and the 10 with the lowest energy were selected for analysis and presentation (Figure 1, Table 1) (*41*). A large, negative Lennard-Jones potential energy (−325.61 ± 17.11 kcal mol^{-1}) indicates reasonable nonbonded geometry of the structure. For the region from residue K1461 to E1565, the root-mean-square deviation (rmsd) values to the mean structure were 0.81 Å for backbone atoms and 1.4 Å for all heavy atoms. The backbone and all heavy atom rmsd values for the well-defined secondary structure elements were 0.66 and 1.21 Å, respectively (SI-2). As expected, higher levels of disorder were found in the ZA loop and BC loop (0.72 Å for backbone atoms and 1.47 Å for all heavy atoms). Both the amino and carboxyl termini showed high internal mobility with no well-defined structure. Therefore, amino terminal residues (1451−1460) and carboxyl terminal residues (1566−1570), including the histidine tag remaining from the pET22b(+) expression vector were not used in rmsd calculations. PROCHECK (*32*) analysis of the 10 NMR structures indicated that >98% of the residues reside in either the most favored regions or additional allowed regions of the Ramachandran plot. No residue is in the disallowed regions (Table 1).

Structure Description. The Brg1 bromodomain structure conforms to previously published bromodomain family members as it contains no β-structure and is 64% helical with a total of six distinct helices (Figure 1) (*25*). The four characteristic α-helices of bromodomain, αZ, αA, αB, and αC, are found in K1461−K1471, F1507−R1515, L1522-F1539, and L1545-E1565. NOE patterns, typical for α-helical conformations, are strongly present in these regions. Further, ^{1}H−^{2}H exchange experiments demonstrate the typical hydrogen bond pattern, between the C′═O of residue *n* and NH of residue *n* + 4. Two short α-helices in ZA loop, helix αZ′ (residues 1483−1486) and helix αA′ (residues 1495−1500), found in the Brg1 bromodomain are conserved in the GCN5 bromodomains. Helix αA′ and helix αZ′ structure are also confirmed by helix-typical NOEs and slowly exchanging NH protons (SI-3).

Brg1 bromodomain α-helices αZ, αA, αB, and αC are arranged in a closely packed, left-handed bundle. The absolute crossing angles between adjacent helices are approximately 20°, with the exception of the N-terminal (αZ)

Table 1: Structural Statistics for the Family of 10 Lowest-Energy Structures[a]

total distance restraints	1183
total NOE restraints	1132
intraresidue ($i - j = 0$)	265
sequential ($\|i - j\| = 1$)	375
medium range ($2 < \|i - j\| < 4$)	264
long range ($\|i - j\| > 5$)	228
hydrogen bonds	51
dihedral angle restraints[b]	
Φ	86
Ψ	86
mean rmsd from idealized covalent geometry	
bond (Å)	0.0008 ± 0.00002
angle (deg)	0.2844 ± 0.0011
improper (deg)	0.1017 ± 0.0043
Lennard-Jones potential energy (kcal mol^{-1})	−325.61 ± 17.11
structural rmsd to the mean coordinates (Å)	
backbone atoms (1461−1565)	0.81
heavy atoms (1461−1565)	1.41
backbone atoms of the secondary structure elements[c]	0.66
heavy atoms of the secondary structure elements[c]	1.21
Ramachandran plot analysis (%)	
residues in the most favorable regions	88.3
additional allowed regions	9.7
generously allowed regions	2.0
residues in disallowed regions	0

[a] None of the structures exhibit distance violations greater than 0.5 Å or dihedral angle violations greater than 5°. [b] The Φ and Ψ angle restraints are generated from secondary structures by TALOS. [c] Residues K1461-K1471, F1507-R1515, L1522-F1539, and L1545-E1565.

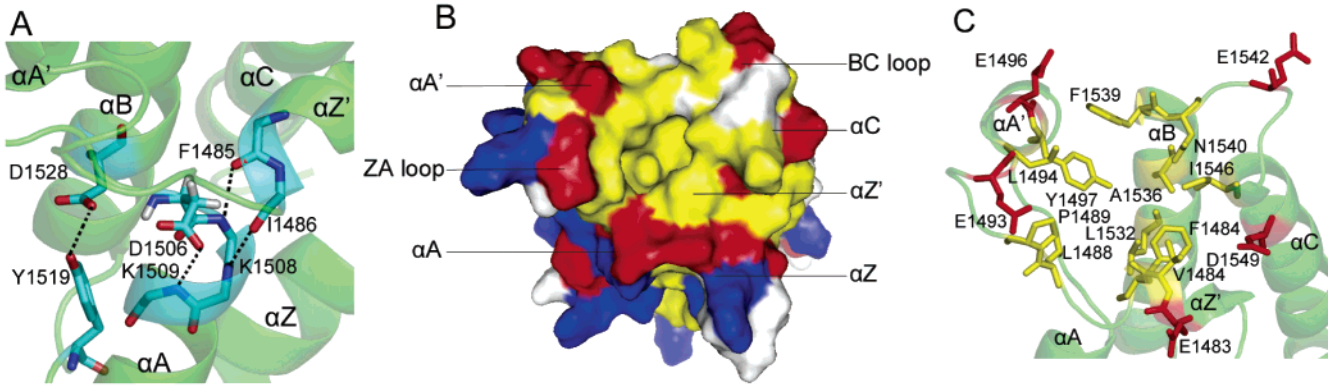

FIGURE 2: Brg1 bromodomain presents a conserved, left-handed topology and hydrophobic acetyllysine binding pocket flanked by acidic residues. (A) Hydrogen bonds cap the αZ′ and αA helices and stabilize the left-handed topology. Brg1 bromodomain represented as green ribbon diagram rotated ($X = 60°$, $Y = 50°$, $Z = 50°$) from Figure 1B and focused on residues 1470−1515, between αZ and αA, i.e., ZA loop. Hydrogen-bonding pairs stabilizing the fold of the left-handed bundle of Brg1 bromodomian include D1528−Y1519, D1506−K1509, I1486−K1508, and F1485−D1507, which are highlighted in cyan. (B) Solvent accessible surface of Brg1 bromodomain, rotated ($X = 60°$, $Y = 0°$, $Z = 100°$) from Figure 1B, with hydrophobic, acidic, and basic residues being yellow, red, and blue, respectively. (C) Side chains from ZA loop, BC loop and αB, αC helices contribute to hydrophobic cavity and flanking acidic mantle, colored as in (B). Residues conserved across the bromodomain family include F1485, L1488, P1489, L1494, E1496, Y1497, A1536, L1532, F1539, N1540, E1542, and I1546 in the Brg1 bromodomain, rotated ($X = 30°$, Y,=30°, $Z = 10°$). E1483 and D1549 are unique to Brg1 and other class I bromodomains. Figures were generated using PyMOL.

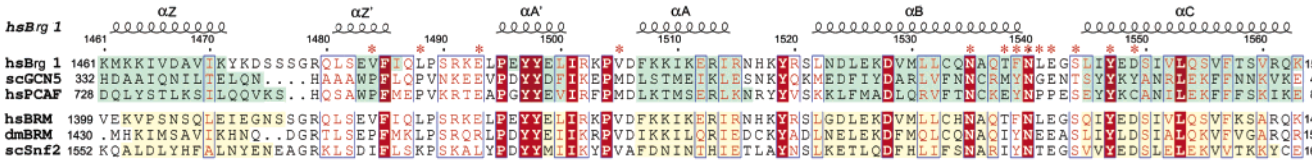

FIGURE 3: Sequence alignment of Brg1 bromodomain with selected bromodomain family members: *sc*GCN5 (1E6I), hsPCAF (1N72) from group VI and *hs*BRM (gi 902046), *dm*BRM (gi 157012) and *sc*Snf2 (gi 6324864) from group I (*24*). Sequences were aligned with ClustalW and then adjusted manually to rectify with published structural data. Brg1 bromodomain residue numbering is indicated above the alignment. Experimentally determined secondary structure, or predicted by Jpred, are shaded in green or yellow, respectively (*48*). Conserved identical or similar residues are shaded in red or blue boxes, respectively. Sequence homology, as determined by BLAST relative to the Brg1 bromodomain is 61% for *sc*GNC5, 53% for *hs*PCAF, 92% for *hs*BRM, 75% for *dm*BRM, and 63% for *sc*Snf2 bromodomains. Residues that are most perturbed by ligand binding are indicated by red asterisks.

and C-terminal (αC) helices, which cross one another at an angle of 47°. The two short helices αZ′ and αA′ are almost orthogonal to each other and positioned perpendicular to the axis of the four-helix bundle, with αZ′ interacting with αB and αC, and αA′ interacting only with helix αB, respectively (Figure 1B).

Hydrogen bonds that cap the helices, anchor the loops, and form the hydrophobic acetyllysine pocket stabilize this unusual left-handed topology (Figure 2A). Backbone carbonyl groups of F1485 and I1486 form hydrogen bonds respectively with backbone amide groups of F1507 and K1508, capping the αA helix and αZ′ helix, and anchoring the long ZA loop. Another helix capping hydrogen bond is formed between the amide group of K1509 and the side chain carboxyl group of the highly conserved D1506 (Figures 2A and 3). Residue Y1519, from the AB loop, and D1528, form helix αB, form a hydrogen bond that contributes to the conformation of the AB loop and incorporates the Y1519 side chain into the hydrophobic core of the protein (Figure 2A). Both residues and the hydrogen bond are highly conserved in GCN5 bromodomomains and other family members (Figure 3) (*42*). The conservation suggests Y1519 hydrogen bonding has an important role in bromodomain structure and function.

A pronounced hydrophobic cavity can be clearly seen on top of the protein (Figure 2B). This cavity is surrounded by the side chains of residues from the long ZA loop, including V1484, F1485, L1488, P1489, L1494, and Y1497 (Figure 2C). Terminal residues from helix αB, including L1532, A1536, and F1539, and I1546 at the end of αC contribute to the cavity (Figure 2C). All these residues are hydrophobic and highly conserved across the bromodomain family (Figure 3). N1540, a highly conserved residue beginning the BC loop, also resides in the cavity. Located at the edge of the hydrophobic cavity, acidic residues including E1483, E1493, E1496, E1542, and D1549 present a negatively charged collar of electrostatic potential around the hydrophobic cavity (Figure 2B,C). Previous studies indicate this cavity is the binding site for lysine-acetylated peptides and demonstrate these conserved acidic residues provide specificity to bromodomain acetyllysine interactions (*42*).

Structure Comparison with Other Bromodomains. Although Brg1 bromodomain shares only about 20−25% sequence identity with those published structures, the overall left-handed four-helix bundle configuration is well conserved (Figures 1B and 4A). The majority of structural deviations are localized in the long ZA loop, including helices αZ′ and αA′. Another feature of Brg1 bromodomain is that its αZ helix is about 4 residues shorter than that of the other bromodomains. Instead of adopting a helix structure found in αZ in previously published bromodomain structures, residues K1473 to S1477 make a turn. Weak HN−HN cross-peaks in NOE spectra further confirmed the structure. This turn tilts the Brg1 αZ about 15°, relative to the *sc*GCN5 αZ

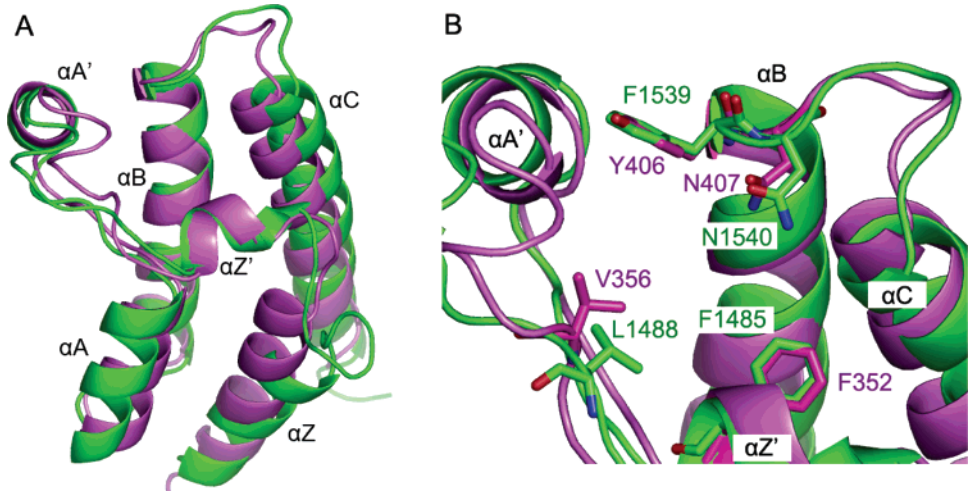

FIGURE 4: Brg1 bromodomain closely resembles the *sc*GCN5 bromodomain in terms of both topology and the configuration of the acetyllysine binding pocket. (A) Cα alignment of the average minimized Brg1 bromodomain and Cα coordinates of *sc*GCN5 bromodomain shown in green and violet, respectively. Rotated ($X = 15°$, $Y = 30°$, $Z = -10°$) from Figure 1B. Relative to *sc*GCN5, the Brg1 bromodomain has a shortened αZ. Concomitantly, αZ in *sc*GCN5 is packed more closely to αC. (B) Side chains for residues implicated in *sc*GCN5 acetyllysine binding specificity are displayed along with corresponding residues in Brg1 bromodomain. Rotated ($X = 10°$, $Y = 30°$, $Z = 10°$) from Figure 1B. The figure was generated with PyMOL.

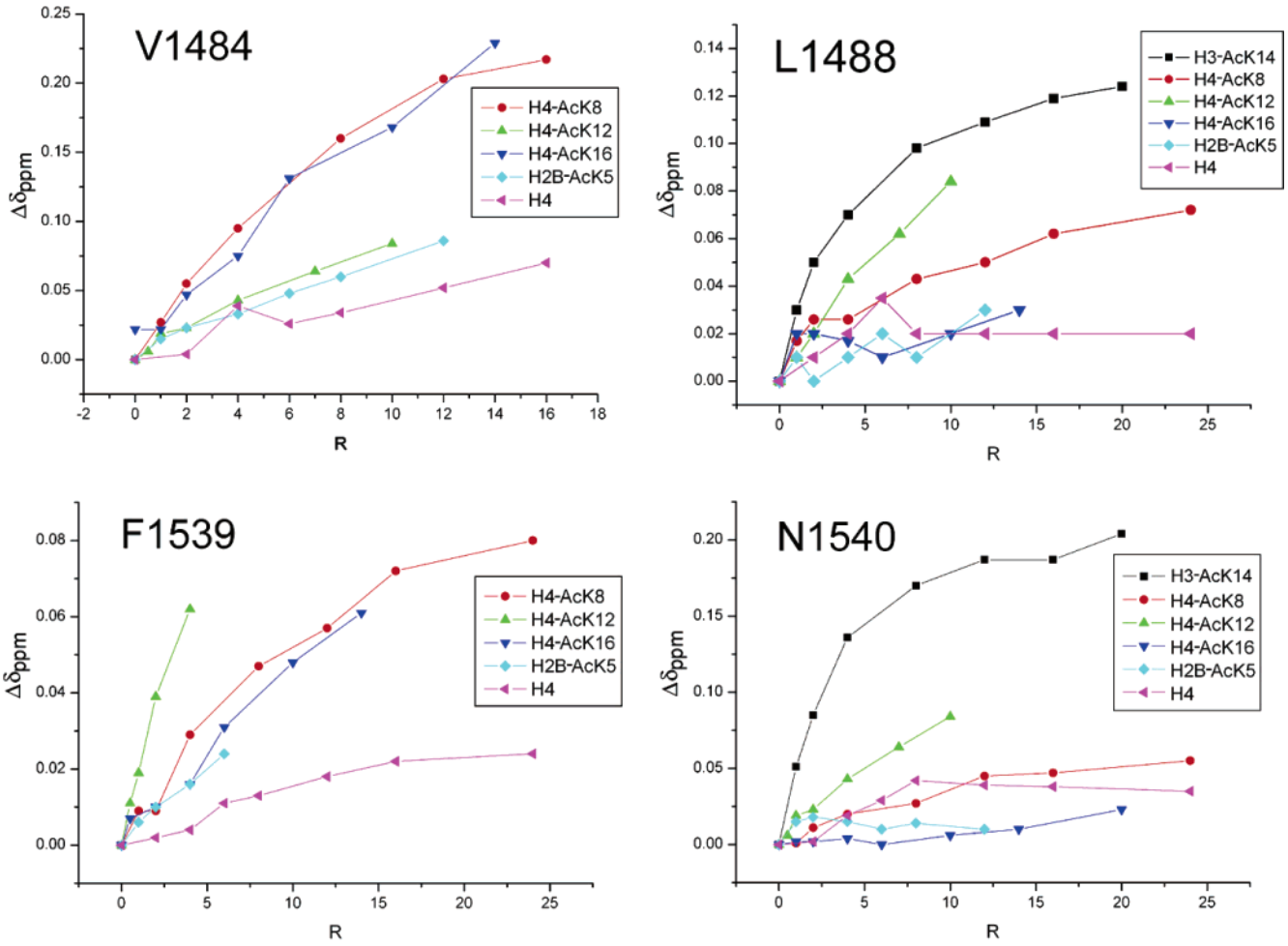

FIGURE 5: Perturbation of the backbone amide chemical shifts of residues V1484, L1488, F1539, and F1540 upon binding of the peptides. R = [peptide]/[bromodomain].

helix, toward the αC helix (Figure 4A). The loss of the carboxyl terminal end of αZ extends the ZA loop and adds additional flexibility along its length.

For further understanding the structural differences, the pairwise backbone RMSDs to *sc*GCN5, *hs*GCN5, *hs*P/CAF, *hs*CBP, *hs*TAF_{II}250-BD1, *hs*TAF_{II}250-BD2 were calculated with the combinatorial extension (CE) method (*38*). The structure of Brg1 bromodomain is most similar to the bromodomain from *sc*GCN5 (rmsd = 2.1 Å), and less similar to the other bromodomains (rmsd about 3

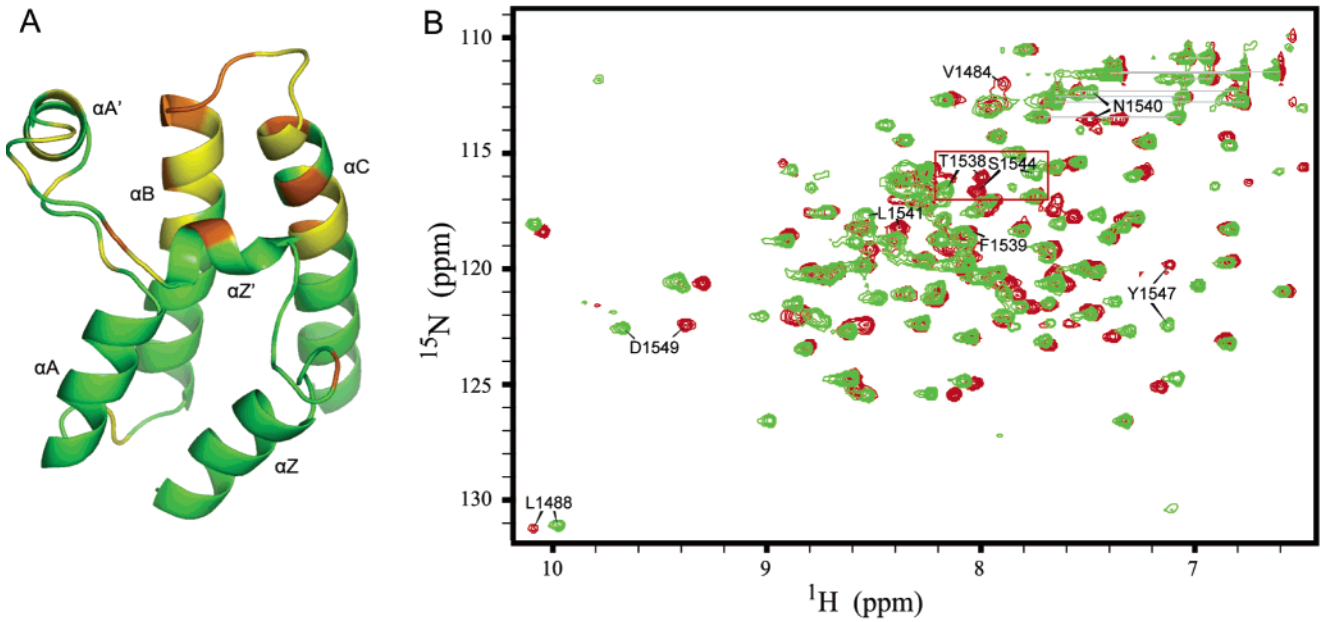

FIGURE 6: (A) Ribbon diagram illustrating the locations of residues most perturbed upon H3−AcK14 binding. Residues with chemical shift changes larger than the mean value plus one standard deviation are orange and residues with chemical shift changes larger than the mean value are yellow. Rotated ($X = 15°$, $Y = 25°$, $Z = -10°$) from Figure 1B. The figure was prepared using the program PyMOL. (B) Superposition of the ^{15}N-HSQC spectra of human Brg1 bromodomain in free (red) and in complex with H3−AcK14 at a 1:20 molar ratio (green). Residues experiencing the greatest chemical shift changes upon complexation are indicated.

Å). Figure 4 shows the backbone superposition of Brg1 on *sc*GCN5.

V1484, L1488, and P1489 of Brg1 bromodomain are highly conserved among class I bromodomains but deviate from other family members (*24*). In other bromodomain family members Pro, Pro, and Val are conserved at these positions in both amino acid sequence and structure (*24*) (Figure 3). These residues are located at the hydrophobic binding surface. Because Pro gives no signal on ^{15}N−^{1}H HSQC spectra, following the V1484 and L1488 signals may reveal the roles they play in bromodomain structures and ligand bindings.

Brg1 Bromodomain Peptide Binding. The 2D ^{1}H−^{15}N HSQC spectrum of the Brg1 bromodomain displays good dispersion of the proton and nitrogen resonances in the amide groups. In this spectrum, 104 out of the 119 backbone amide resonances were assigned. To investigate the binding property of Brg1 bromodomain to acetylated peptides, NMR perturbation experiments were carried out. Peptides H4−AcK8, H4−AcK12, H4−AcK16, H3−AcK14, and H2B−AcK5 and a H3 peptide with an Arg 17 to Ala mutation, H3−R17/A, were titrated against ^{15}N-labled Brg1 bromodomain. A ^{15}N−^{1}H HSQC spectrum was recorded at each titration point of the peptides, to 20 molar excess of peptide to Brg1 bromodomain. The chemical shift changes for amide resonances, between free and the final bound states, were calculated and plotted against the Brg1 residue number (SI-4). Perturbations upon binding were small ($\Delta\delta$HN < 0.22 ppm; $\Delta\delta$N < 1.2 ppm; weighed average $\Delta\delta$ < 0.3 ppm) but significant. V1484, L1488, F1539, and N1540 demonstrated the largest chemical shift changes and were plotted in Figure 5. Each titrated peptide demonstrated a markedly unique effect on the chemical shifts under analysis with unacetylated H4 peptide causing no obvious chemical shift changes (Figure 5).

In our experiments, H3−AcK14 had the greatest effect on the chemical shifts. During H3−Ack14 titration, the NH cross-peak of V1484 and F1539 completely disappeared due to line broadening at low peptide concentration (R = 1:1). Additional residues T1538, S1544, L1541, Y1547, and D1549 experienced large chemical shift changes not seen with the other peptides in our study (Figure 6B). Figure 5A illustrates the locations of the residues most perturbed upon H3−AcK14 binding. The overall perturbation patterns of H4−AcK8 and H4−AcK12 are similar and a few but significant chemical shift changes were observed (SI-4). H4−AcK16 and H2B-AcK5 also induce similar chemical shift changes but to a less magnitude (Figure 5).

Dissociation constants (K_D) were calculated using the average of four representative residues. The estimated K_D's for H3−AcK14, H4−AcK8, and H4−AcK12 are 1.2, 4.0, and 3.6 mM, respectively. For H4−AcK16 and H2B-AcK5, no K_D can be estimated because the binding affinities are much lower than we could determine experimentally.

Model of the Brg1 Bromodomain H3−AcK14 Complex. We choose 1E6I as a template for our molecular dynamics (MD) simulation model because, when compared to the Brg1 bromodomain, the *sc*GCN5 bromodomain has the lowest Cα rmsd deviation among determined structures of the bromodomain family. The model shows four significant interactions (Figure 7A,B). The H3−AcK14 acetyl group is inserted into the hydrophobic slot surrounded by V1484, F1485, L1488, F1539, and I1546. The carbonyl group of *N*-acetyllysine forms a hydrogen bond with N1540. The side chain NH_2 of Arg 17 forms a hydrogen bond with the backbone carbonyl of T1538. Pro 16 forms hydrophobic interactions with L1494. H4−AcK16, a substrate of the *sc*GCN5 bromodomain, is also a potential ligand for the Brg1 bromodomain. However, using identical MD parameters, which generated the modeled Brg1 bromodomain H3−AcK14 complex, no plausible complex could be found.

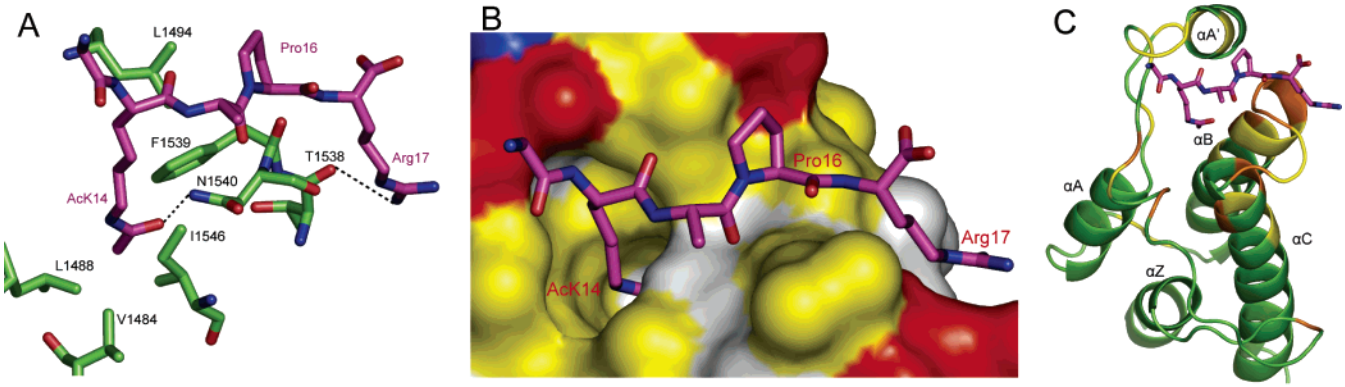

FIGURE 7: Brg1 bromodomain in complex with peptide H3−AcK14. (A) Sticks diagram depicting the hydrophobic and hydrogen bond interactions between Brg1 and the acetylated peptide. Rotated ($X = 15°$, $Y = -30°$, $Z = 100°$) from Figure 1B. Hydrogen bonds are shown with dotted lines. Peptide side chains are violet. Protein side chains are green. (B) "Top" view of the molecular surface colored by hydrophobic potential (yellow marks hydrophobic residues; red, negative residues; blue, positive residues; white, polar residues). Rotated ($X = 30°$, $Y = -30°$, $Z = 80°$) from Figure 1B. The acetylated lysine side chain fits into the deep slot. (C) Ribbon representation in the same orientation as in (B), showing the peptide position relative to residues perturbed most greatly (orange) and less greatly (yellow) upon binding. The color scheme is the same as in (B). Molecular graphics were generated with the program PyMOL.

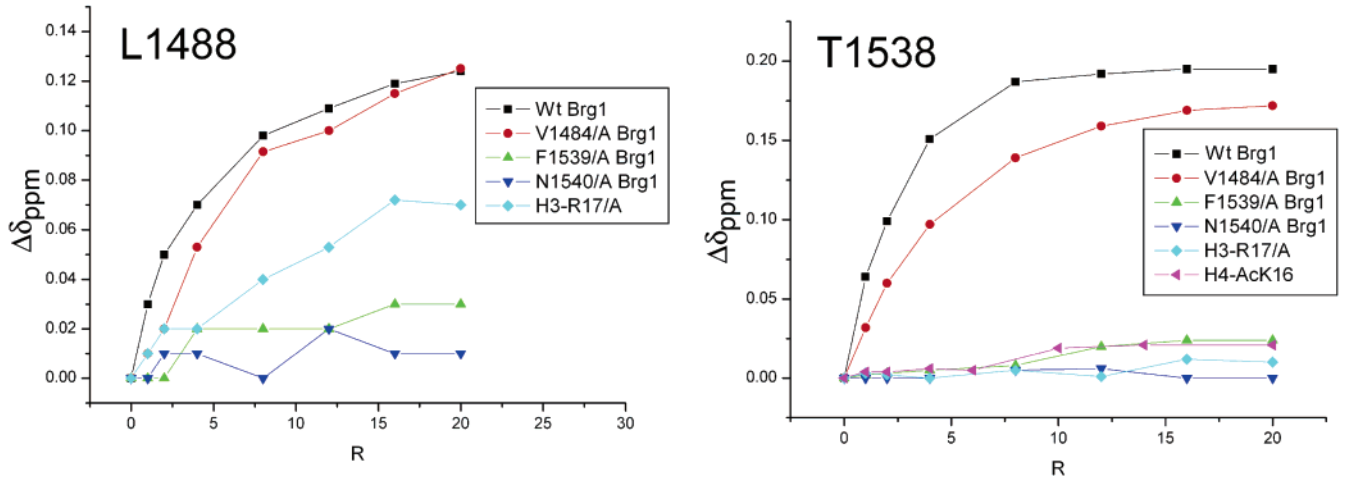

FIGURE 8: Brg1 bromodomain residues F1539 and N1540 and H3 residue Arg 17 are critical to the Brg1 bromodomain H3−AcK14 binding. Chemical shift perturbations of residue L1488 and T1538 on wild-type and mutant Brg1 bromodomains titrated with H3−AcK14, and H3−R17/A effects on wild-type Brg1 bromodomain. R = [peptide]/[bromodomain].

Mutational Analysis. We mutagenized both the H3−AcK14 peptide and Brg1 bromodomain to determine which residues are significant for binding. Mutations include V1484/A, F1539/A, and N1540/A on the Brg1 bromodomain and a R17/A mutation in H3−AcK14. ^{15}N-HSQC spectra were collected using mutagenized Brg1 bromodomain titrated with H3−AcK14 peptide. The V1484/A mutation does not affect binding, as the residue amide resonances shift like wild-type Brg1 bromodomain in response to H3−AcK14 peptide titration (Figure 8). With the same titration conditions, both F1539/A and N1540/A radically reduce the residue amide resonance shifts relative to wild-type Brg1 bromodomain, as illustrated by L1488 and T1538, indicating their importance in H3−AcK14 binding (Figure 8). The mutagenized R17/A H3−AcK14 peptide causes no significant chemical shift changes on the ^{15}N-HSQC spectra, as observed via T1538 and S1544 (Figure 9B).

DISCUSSION

Human brahma-related gene 1 (Brg1) is a highly conserved, multidomain protein essential for gene regulation in a chromatin environment. Despite intense biological studies and a wealth of biochemical data, Brg1 lacks direct structural information. The Brg1 bromodomain has been implicated in the recruitment of the SWI/SNF complex to chromatin, which is consistent with its ability to bind acetyllysine (*29*). The Brg1 bromodomain represents group I bromodomains that are associated with ATP-dependent chromatin-remodeling activity, and no structural information is known (*24*, *43*). Here we report the solution structure of Brg1 bromodomain, the first representative of group I, ATPase associated bromdomain.

The Brg1 bromodomain conserves the left-handed, four-helix bundle topology found in other bromodomain family members. Results of 3D ^{15}N-edited and ^{13}C-edited NOESY experiments and ^{1}H−^{2}H exchange experiments define the four-helix bundle αZ, αA, αB, and αC, and the two short helices αZ′ and αA′ in the long ZA loop, all of which are conserved in *sc*GCN5 and other bromodomain family members (SI-3, Figures 1 and 4A). Highly conserved residues, including F1485, D1506, Y1519, and D1528, and the hydrogen bonds between them, configure the left-handed topology of the four principle helices (Figures 2A and 3). At the top of this four-helix bundle resides the hydrophobic acetyllysine binding pocket, which is collared by a negative electrostatic potential (Figure 2B,C). The Brg1 bromodomain

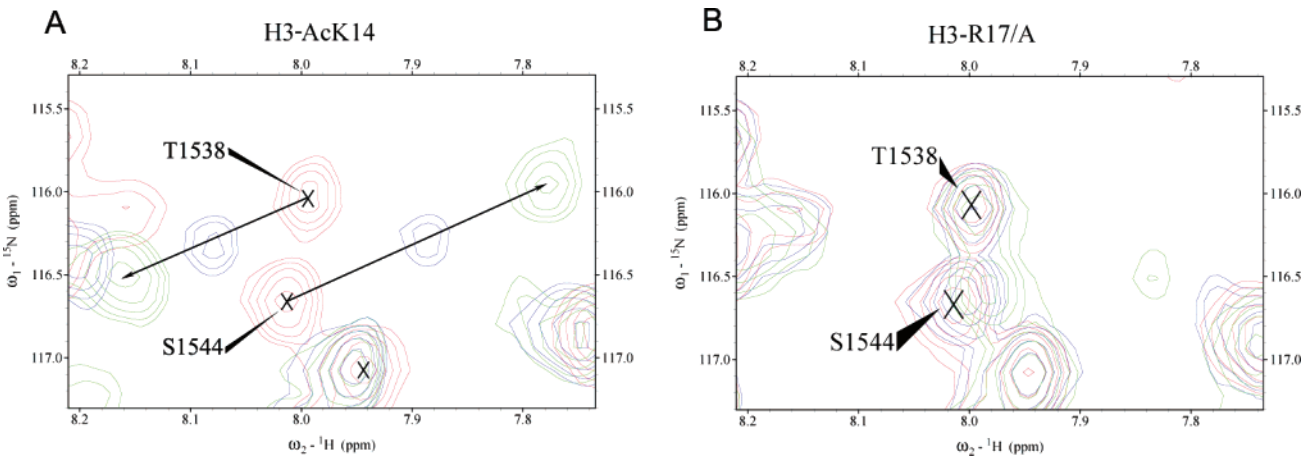

FIGURE 9: H3 residue Arg 17 is critical for Brg1 bromodomain H3−AcK14 binding. (A) Superimposed region of the 2D ^{15}N-HSQC (~0.3 mM) of Brg1 bromodomain complexed to H3−AcK14 or (B) in complex with R17/A H3−AcK14. Brg1 bromodomain free form is red, $R = 4$ is violet and $R = 16$ is green. $R =$ [peptide]/[bromodomain].

Table 2: Peptides Used for Binding to Brg1 Bromodomain

name	sequence	description
H4	SGRGKGGKGLGK	human H4 histone residues 1−12
H4−AcK8	SGRGKGG−AcK[a]−GLGK	K8-acetylated human H4 histone residues 1−12
H4−AcK12	GKGLG−AcK−GGAKR	K12-acetylated human H4 histone residues 7−17
H4−AcK16	GGA−AcK−RHRK	K16-acetylated human H4 histone residues13−20
H3−AcK14	KSTGG−AcK−APRK	K14-acetylated human H3 histone residues 9−18
H3−R17/A	KSTGG−AcK−APAK	R17/A mutant of H3−AcK14
H2B−AcK5	SDPA−AcK−SAPAPKK	K5-acetylated human H2B histone residues 1−12

[a] AcK represents acetylated lysine.

maintains all the standard features except one difference in the αZ helix. The Brg1 bromodomain αZ helix, as determined by TALOS calculation and NOE restraints, is 4 residues shorter relative to previously published bromodomain structures (Figures 3 and 4A and SI-3).

Using NMR perturbation studies, we demonstrate the Brg1 bromodomain binds acetyllysine in the context of histone tails, with no comparable affinity for unacetylated peptides. The estimated dissociation constants (K_D) for acetylated histone peptides H4−AcK8 and H4−AcK12 are 4.0 and 3.6 mM, respectively. The dominant substrate is H3−AcK14 ($K_D \approx 1.2$ mM). H3−AcK14 titration induced a greater number of distinct chemical shift changes to Brg1 bromodomain (Figures 5, 6B, and 9). Most of the residues perturbed mapped to the acetyllysine binding pocket composed of ZA and BC loops and the carboxyl and amino termini of helices αB and αC, respectively (Figures 6A and 7C). Other lysine-acetylated peptides that were assayed caused variable and generally weak perturbations (Figure 5, SI-4).

We were interested in the potential interactions which provide the selectivity of the Brg1 bromodomain for histone H3−AcK14. For example, N407 of *sc*GCN5 (Figures 3 and 4B) is responsible for *N*-acetyllysine binding and this interaction is highly conserved among all classes of bromodomains (*44*). However, ligand selectivity of bromodomains is a composite of the acetyllysine binding pocket and residues flanking both sides of the pocket (*45*). Specifically, the negative charge near the binding pocket of *hs*GCN5 bromodomain favor the binding of basic peptides and discriminate against negatively charged ligands (*42*). In another example, in the selective binding of H4−AcK16 by *sc*GCN5, residue His at K+2 and Arg at K+3 are essential for binding specificity, where K defines the position of the acetylated lysine (*44*).

In our study, H3−AcK14 is the favored substrate of the Brg1 bromodomain, but without a complex of the Brg1 bromodomain and H3−AcK14, we could not identify the structural requirements for the interaction. From the published bromodomain structures the *sc*GCN5 bromodomain has the highest resolution, highest sequence homology, lowest Cα rmsd and highest structural homology in the acetyllysine binding domain, when compared to the Brg1 bromodomain (Figures 3 and 4). Further, the ligand H4−AcK16, found in the *sc*GCN5 H4−AcK16 complex, has an Arg at K+3 homologous to Arg 17 in H3−AcK14, the favored Brg1 bromodomain substrate (Table 2). With so many common features the bromodomains from *sc*GCN5 and Brg1 could share similar ligand selectivities. Therefore, we used the crystal structure of *sc*GCN5 in complex with H4−AcK16 (PDB ID 1E6I), which were generously donated by D. J. Owen et al. (*44*), as a template for our molecular dynamics (MD) simulations.

Our Brg1 bromodomain H3−AcK14 complex model yields insights into the molecular mechanisms of chemical shift perturbation experiments (Figure 7). In the complex model, Arg 17 in H3−AcK14 forms a hydrogen bond with T1538 (Figure 7A), reflected by a substantial chemical shift change of T1538 upon binding (Figure 9A). When this arginine is mutated to alanine, no chemical shift change can be observed of T1538 upon binding of the mutated H3−AcK14 (Figures 8 and 9B). This result is in accordance with the complex model. As a consequence, the significant perturbations on other residues were also reduced in intensity or absent.

The complex model also confirms the important role of the highly conserved residues N1540 and F1539. The model shows a hydrogen bond between the carbonyl group of *N*-acetyl in H3−AcK14 and the side chain amide in N1540 and hydrophobic interactions between the acetyllysine and F1539. When these two residues are substituted by alanines, Brg1 bromodomain no longer binds to H3−AcK14 (Figure 8). This is the direct evidence, from the model and confirmed by experiment, that the highly conserved N1540 and type conserved F1539 play critical roles in acetylated lysine peptide bindings.

The apo Brg1 bromodomain structure, model Brg1 bromodomain H3−Ack14 complex, and ^{15}N-HSQC perturbation studies we present shed light on the potential structural and molecular details for substrate specificity of Brg1 bromodomain and perhaps give insights into the acetyllysine binding potential of group I, ATPase associated, bromdomains. Interaction of bromodomains with acetyllysine is reminiscent of specific recognition of phosphorylated residues by SH2 domain (*46*). The recognition of acetylated histones by bromodomain proteins is regarded as a major part of histone code of eukaryotic gene activation. Agalioti et al. reported that during the activation of INF-β gene, acetylation of histone H4 K8 mediated recruitment of the SWI/SNF complex and gene activation (*29*). To explain this, they provided a model of sequential binding of HATs, SWI/SNF, and basal transcription factors for ordered recruitments of coactivator complexes and consequent INF-β gene activation. The results from our NMR perturbation studies provide some structural basis for this model. We show that the Brg1 bromodomain recognizes H4−AcK8 and H4−AcK12 but not unacetylated H4 (Figure 5). However, it is surprising we find the Brg1 bromodomain binds H3−AcK14 with higher affinity because Agalioti et al. reported that acetylated peptides from the N-termini of histone H3 did not affect the recruitment of Brg1 in their competition assays (*29*). However, Kouskouti et al. recently reported Brg1 bromodomain could interact with K9/K14-acetylated H3 peptides in their pull down assay (*47*). Our titration of the Brg1 bromodomain with H3−AcK14 corroborates this result. Ahmed et al. observed that Swi2/Snf2 bromodomain swapped into yGCN5 was able to bind to acetylated histone H3 (*28*). If the Brg1 bromodomain is representative of other group I bromodomains, then it could be possible for Snf2 bromodomain to interact with acetylated histone H3, leading to ordered coactivator recruitment deciphering of the histone code.

ACKNOWLEDGMENT

We thank Dr. F. Delaglio and Prof. A. Bax for providing the software NMRPipe, Prof. T. D. Goddard and Prof. D. G. Kneller for providing Sparky, Prof. A. T. Brünger for providing the program CNS, Dr. R. Koradi, and Prof. K. Wüthrich for providing MOLMOL (*33*), Dr. W. L. Delano for providing PyMOL, Prof. W. F. van Gunstern, for providing GROMOS96 package (*40*), and Prof. D. J. Owen for providing the coordinates of the crystal structure of *sc*GCN5 in complex with H4−AcK16 (PDB ID 1E6I) (*44*).

SUPPORTING INFORMATION AVAILABLE

Number of NOE restraints per residue used in structure calculation (SI-1), backbone atom and all heavy atom average rmsd values for each residue for the ensemble of 10 bromodomain structures (SI-2), summary of sequential and medium-range NOE patterns observed in Brg1 bromodomain (SI-3), combined chemical shift perturbations to the Brg1 bromodomain by titration of H4−AcK8 (A), H4−AcK12 (B), and H3−AcK14 (C) peptides (SI-4). This material is available free of charge via the Internet at http://pubs.acs.org.

REFERENCES

1. Eisen, J. A., Sweder, K. S., and Hanawalt, P. C. (1995) Evolution of the SNF2 family of proteins: subfamilies with distinct sequences and functions. *Nucleic Acids Res. 23*, 2715−23.
2. Vignali, M., Hassan, A. H., Neely, K. E., and Workman, J. L. (2000) ATP-dependent chromatin-remodeling complexes. *Mol. Cell Biol. 20*, 1899−910.
3. Logie, C., and Peterson, C. L. (1997) Catalytic activity of the yeast SWI/SNF complex on reconstituted nucleosome arrays. *Embo. J. 16*, 6772−82.
4. Stern, M., Jensen, R., and Herskowitz, I. (1984) Five SWI genes are required for expression of the HO gene in yeast. *J. Mol. Biol. 178*, 853−68.
5. Carlson, M., Osmond, B. C., and Botstein, D. (1981) Genetic evidence for a silent SUC gene in yeast. *Genetics 98*, 41−54.
6. Tamkun, J. W., Deuring, R., Scott, M. P., Kissinger, M., Pattatucci, A. M., Kaufman, T. C., and Kennison, J. A. (1992) brahma: a regulator of *Drosophila* homeotic genes structurally related to the yeast transcriptional activator SNF2/SWI2. *Cell 68*, 561−72.
7. Chiba, H., Muramatsu, M., Nomoto, A., and Kato, H. (1994) Two human homologues of *Saccharomyces cerevisiae* SWI2/SNF2 and *Drosophila* brahma are transcriptional coactivators cooperating with the estrogen receptor and the retinoic acid receptor. *Nucleic Acids Res. 22*, 1815−20.
8. Kingston, R. E., Bunker, C. A., and Imbalzano, A. N. (1996) Repression and activation by multiprotein complexes that alter chromatin structure. *Genes Dev. 10*, 905−20.
9. Kadam, S., and Emerson, B. M. (2003) Transcriptional specificity of human SWI/SNF BRG1 and BRM chromatin remodeling complexes. *Mol. Cell 11*, 377−89.
10. Sif, S. (2004) ATP-dependent nucleosome remodeling complexes: enzymes tailored to deal with chromatin. *J. Cell Biochem. 91*, 1087−98.
11. Pal, S., Vishwanath, S. N., Erdjument-Bromage, H., Tempst, P., and Sif, S. (2004) Human SWI/SNF-associated PRMT5 methylates histone H3 arginine 8 and negatively regulates expression of ST7 and NM23 tumor suppressor genes. *Mol. Cell Biol. 24*, 9630−45.
12. Pal, S., Yun, R., Datta, A., Lacomis, L., Erdjument-Bromage, H., Kumar, J., Tempst, P., and Sif, S. (2003) mSin3A/histone deacetylase 2- and PRMT5-containing Brg1 complex is involved in transcriptional repression of the Myc target gene cad. *Mol. Cell Biol. 23*, 7475−87.
13. Hendricks, K. B., Shanahan, F., and Lees, E. (2004) Role for BRG1 in cell cycle control and tumor suppression. *Mol. Cell Biol. 24*, 362−76.
14. Strobeck, M. W., Knudsen, K. E., Fribourg, A. F., DeCristofaro, M. F., Weissman, B. E., Imbalzano, A. N., and Knudsen, E. S. (2000) BRG-1 is required for RB-mediated cell cycle arrest. *Proc. Natl. Acad Sci. U.S.A. 97*, 7748−53.
15. Zhang, H. S., Gavin, M., Dahiya, A., Postigo, A. A., Ma, D., Luo, R. X., Harbour, J. W., and Dean, D. C. (2000) Exit from G1 and S phase of the cell cycle is regulated by repressor complexes containing HDAC-Rb-hSWI/SNF and Rb-hSWI/SNF. *Cell 101*, 79−89.
16. Reisman, D. N., Sciarrotta, J., Wang, W., Funkhouser, W. K., and Weissman, B. E. (2003) Loss of BRG1/BRM in human lung cancer cell lines and primary lung cancers: correlation with poor prognosis. *Cancer Res. 63*, 560−6.
17. Wong, A. K., Shanahan, F., Chen, Y., Lian, L., Ha, P., Hendricks, K., Ghaffari, S., Iliev, D., Penn, B., Woodland, A. M., Smith, R., Salada, G., Carillo, A., Laity, K., Gupte, J., Swedlund, B., Tavtigian, S. V., Teng, D. H., and Lees, E. (2000) BRG1, a component of the SWI-SNF complex, is mutated in multiple human tumor cell lines. *Cancer Res. 60*, 6171−7.
18. Murphy, D. J., Hardy, S., and Engel, D. A. (1999) Human SWI-SNF component BRG1 represses transcription of the c-fos gene. *Mol. Cell Biol. 19*, 2724−33.

19. Strobeck, M. W., DeCristofaro, M. F., Banine, F., Weissman, B. E., Sherman, L. S., and Knudsen, E. S. (2001) The BRG-1 subunit of the SWI/SNF complex regulates CD44 expression. *J. Biol. Chem. 276*, 9273−8.
20. Gebuhr, T. C., Kovalev, G. I., Bultman, S., Godfrey, V., Su, L., and Magnuson, T. (2003) The role of Brg1, a catalytic subunit of mammalian chromatin-remodeling complexes, in T cell development. *J. Exp. Med. 198*, 1937−49.
21. Fry, C. J., and Peterson, C. L. (2001) Chromatin remodeling enzymes: who's on first? *Curr. Biol. 11*, R185−97.
22. Biggs, J. R., Yang, J., Gullberg, U., Muchardt, C., Yaniv, M., and Kraft, A. S. (2001) The human brm protein is cleaved during apoptosis: the role of cathepsin G. *Proc. Natl. Acad Sci. U.S.A. 98*, 3814−9.
23. Haynes, S. R., Dollard, C., Winston, F., Beck, S., Trowsdale, J., and Dawid, I. B. (1992) The bromodomain: a conserved sequence found in human, *Drosophila* and yeast proteins. *Nucleic Acids Res. 20*, 2603.
24. Jeanmougin, F., Wurtz, J. M., Le Douarin, B., Chambon, P., and Losson, R. (1997) The bromodomain revisited. *Trends Biochem. Sci. 22*, 151−3.
25. Dhalluin, C., Carlson, J. E., Zeng, L., He, C., Aggarwal, A. K., and Zhou, M. M. (1999) Structure and ligand of a histone acetyltransferase bromodomain. *Nature 399*, 491−6.
26. Strahl, B. D., and Allis, C. D. (2000) The language of covalent histone modifications. *Nature 403*, 41−5.
27. Turner, B. M. (2000) Histone acetylation and an epigenetic code. *Bioessays 22*, 836−45.
28. Hassan, A. H., Prochasson, P., Neely, K. E., Galasinski, S. C., Chandy, M., Carrozza, M. J., and Workman, J. L. (2002) Function and selectivity of bromodomains in anchoring chromatin-modifying complexes to promoter nucleosomes. *Cell 111*, 369−79.
29. Agalioti, T., Chen, G., and Thanos, D. (2002) Deciphering the transcriptional histone acetylation code for a human gene. *Cell 111*, 381−92.
30. Cornilescu, G., Delaglio, F., and Bax, A. (1999) Protein backbone angle restraints from searching a database for chemical shift and sequence homology. *J. Biomol. NMR 13*, 289−302.
31. Brunger, A. T., Adams, P. D., Clore, G. M., DeLano, W. L., Gros, P., Grosse-Kunstleve, R. W., Jiang, J. S., Kuszewski, J., Nilges, M., Pannu, N. S., Read, R. J., Rice, L. M., Simonson, T., and Warren, G. L. (1998) Crystallography & NMR system: A new software suite for macromolecular structure determination. *Acta Crystallogr. D Biol. Crystallogr 54*, 905−21.
32. Laskowski, R. A., Rullmannn, J. A., MacArthur, M. W., Kaptein, R., and Thornton, J. M. (1996) AQUA and PROCHECK-NMR: programs for checking the quality of protein structures solved by NMR. *J. Biomol. NMR 8*, 477−86.
33. Koradi, R., Billeter, M., and Wuthrich, K. (1996) MOLMOL: a program for display and analysis of macromolecular structures. *J. Mol. Graph 14*, 51−5, 29−32.
34. Tochio, H., Zhang, Q., Mandal, P., Li, M., and Zhang, M. (1999) Solution structure of the extended neuronal nitric oxide synthase PDZ domain complexed with an associated peptide. *Nature Struct Biol. 6*, 417−21.
35. Lian, L. Y., Barsukov, I. L., Sutcliffe, M. J., Sze, K. H., and Roberts, G. C. (1994) Protein-ligand interactions: exchange processes and determination of ligand conformation and protein-ligand contacts. *Methods Enzymol. 239*, 657−700.
36. Liu, D., Prasad, R., Wilson, S. H., DeRose, E. F., and Mullen, G. P. (1996) Three-dimensional solution structure of the N-terminal domain of DNA polymerase beta and mapping of the ssDNA interaction interface. *Biochemistry 35*, 6188−200.
37. Hu, H. Y., Horton, J. K., Gryk, M. R., Prasad, R., Naron, J. M., Sun, D. A., Hecht, S. M., Wilson, S. H., and Mullen, G. P. (2004) Identification of small molecule synthetic inhibitors of DNA polymerase beta by NMR chemical shift mapping. *J. Biol. Chem. 279*, 39736−44.
38. Shindyalov, I. N., and Bourne, P. E. (1998) Protein structure alignment by incremental combinatorial extension (CE) of the optimal path. *Protein Eng. 11*, 739−47.
39. Dunbrack, R. L., Jr., and Karplus, M. (1993) Backbone-dependent rotamer library for proteins. Application to side-chain prediction. *J. Mol. Biol. 230*, 543−74.
40. Van Gunstern, W. F., Billeter, S. R., Eising, A. A., Hunenberger, P. H., Kruger, P., Mark, A. E., Scott, W. R., and Tironi, I. G. (1996) *Biomolecular simulation: The GROMOS96 manual and user guide*, Vdf Hochschulverlag, Zurich.
41. Tolkatchev, D., Shaykhutdinov, R., Xu, P., Plamondon, J., Watson, D. C., Young, N. M., and Ni, F. (2006) Three-dimensional structure and ligand interactions of the low molecular weight protein tyrosine phosphatase from *Campylobacter jejuni*. *Protein Sci. 15*, 2381−94.
42. Hudson, B. P., Martinez-Yamout, M. A., Dyson, H. J., and Wright, P. E. (2000) Solution structure and acetyl-lysine binding activity of the GCN5 bromodomain. *J. Mol. Biol. 304*, 355−70.
43. Sudarsanam, P., and Winston, F. (2000) The Swi/Snf family nucleosome-remodeling complexes and transcriptional control. *Trends Genet. 16*, 345−51.
44. Owen, D. J., Ornaghi, P., Yang, J. C., Lowe, N., Evans, P. R., Ballario, P., Neuhaus, D., Filetici, P., and Travers, A. A. (2000) The structural basis for the recognition of acetylated histone H4 by the bromodomain of histone acetyltransferase gcn5p. *Embo. J. 19*, 6141−9.
45. Zeng, L., and Zhou, M. M. (2002) Bromodomain: an acetyl-lysine binding domain. *FEBS Lett. 513*, 124−8.
46. Yang, X. J. (2004) Lysine acetylation and the bromodomain: a new partnership for signaling. *Bioessays 26*, 1076−87.
47. Kouskouti, A., and Talianidis, I. (2005) Histone modifications defining active genes persist after transcriptional and mitotic inactivation. *Embo. J. 24*, 347−57.
48. Cuff, J. A., Clamp, M. E., Siddiqui, A. S., Finlay, M., and Barton, G. J. (1998) JPred: a consensus secondary structure prediction server. *Bioinformatics 14*, 892−3.

BI0611208